

Article

Steric Effects of Alkyl Substituents at *N*-Donor Bidentate Amines Direct the Nuclearity, Bonding and Bridging Modes in Isothiocyanato-Copper(II) Coordination Compounds

Franz A. Mautner ^{1,*}, Roland C. Fischer ², Ana Torvisco ² , Maher M. Henary ³, Andrew Milner ⁴, Hunter DeVillier ⁴, Tolga N. V. Karsili ⁴, Febee R. Louka ⁴ and Salah S. Massoud ^{4,*} 

¹ Institut für Physikalische and Theoretische Chemie, Technische Universität Graz, A-8010 Graz, Austria

² Institut für Anorganische Chemie, Technische Universität Graz, Stremayrgasse 9/V, A-8010 Graz, Austria; roland.fischer@tugraz.at (R.C.F.); ana.torviscogomez@tugraz.at (A.T.)

³ Department of Chemistry and Biochemistry, University of California, Los Angeles, CA 90095-1569, USA; henary@chem.ucla.edu

⁴ Department of Chemistry, University of Louisiana at Lafayette, P.O. Box 43700, Lafayette, LA 70504, USA; arm0128@louisiana.edu (A.M.); hjd1005@louisiana.edu (H.D.); tolga.karsili@louisiana.edu (T.N.V.K.); frl6631@louisiana.edu (F.R.L.)

* Correspondence: mautner@tugraz.at (F.A.M.); ssmassoud@louisiana.edu (S.S.M.); Tel.: +43-316-4873-8234 (F.A.M.); +1-337-482-5672 (S.S.M.)

Received: 1 December 2018; Accepted: 10 January 2019; Published: 13 January 2019



Abstract: A series of Cu(II)-isothiocyanato coordination compounds derived from sterically hindered *N*-donor diamines were synthesized and characterized: *catena*-[Cu(Me₃en)(μ-NCS)(NCS)] (1), *catena*-[Cu(NEt₂Meen)(μ-NCS)(NCS)] (2), *catena*-[Cu(N,N,2,2-Me₄pn)(μ-NCS)(NCS)] (3), the dimeric [Cu₂(N,N'-isp₂en)₂(μ-NCS)₂(NCS)₂] (4) and the monomeric compound [Cu(N,N'-*t*-Bu₂en)(NCS)₂] (5), where Me₃en = *N,N,N'*-trimethylethylenediamine, NEt₂Meen = *N,N*-diethyl-*N'*-methylethylenediamine, *N,N*,2,2-Me₄pn = *N,N*,2,2-tetramethylpropylenediamine, *N,N'*-isp₂en = *N,N'*-diisopropylethylenediamine and *N,N'*-*t*-Bu₂en = *N,N'*-di(*tert*-butyl)ethylenediamine. The coordination compounds were characterized by elemental microanalyses, IR, and UV–Vis spectroscopy as well as single crystal X-ray crystallography. Density Functional Theory (DFT) was used to evaluate the role of steric effects in compounds 4 and 5 and how this may affect the adaptation of a specific geometry, NCS-bonding mode, and the dimensionality of the resulting coordination compound.

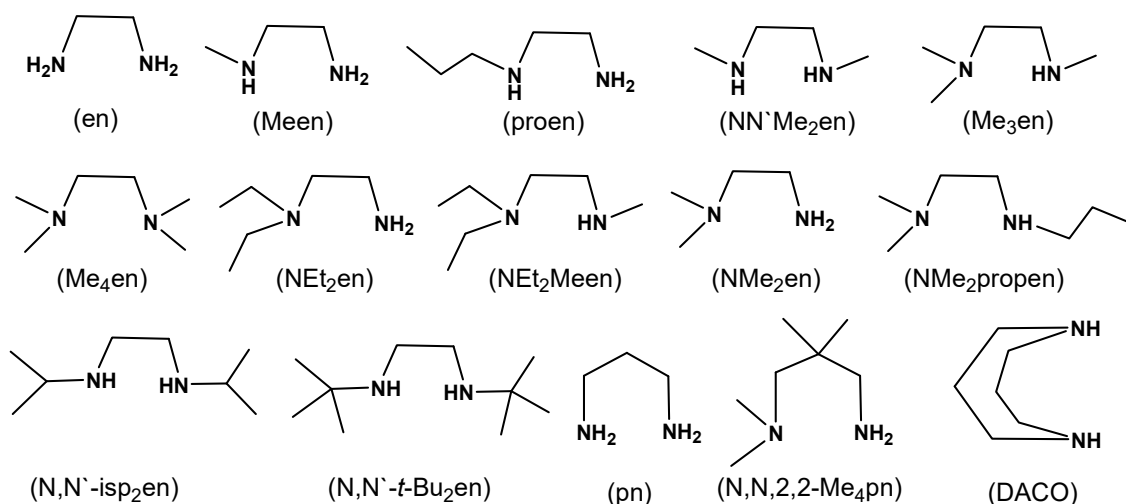
Keywords: coordination compounds; coordination polymers; copper; isothiocyanate; crystal structure; DFT calculations

1. Introduction

Pseudohalides are a class of compounds that are able to simultaneously bind two or more metal ions leading to the formation of di- or poly-nuclear coordination compounds of different nuclearity and clusters, and coordination polymers (CPs) of different dimensionality (1D, 2D, 3D) and topology [1–10]. However, the formation of these compounds depends largely on a number of factors which include the electronic nature and oxidation state of the metal ion, the nature of the coordinated ancillary co-ligand(s), its skeletal structure, and the steric hindrance imposed by the blocking co-ligand(s) surrounding the central metal ion [11,12]. Steric effects caused by the coordinating blocking ligands in coordination compounds have been reported to produce a dramatic effect on the structural and magnetic behavior of pseudohalide coordination compounds [1–11,13–16] but also in the biological catalytic reactions of the P–O bond cleavage in DNA and phosphodiester hydrolysis [17–20].

Isothiocyanato coordination compounds are considered as among the most studied systems in coordination chemistry due to the diverse bonding properties of the NCS^- ion as an ambidentate and bridging ligand that can bind two or more metal ions simultaneously as well as its ability to propagate magnetic interaction between bridged paramagnetic metal ions. In general, several bonding modes were reported in bridging-isothiocyanato-polynuclear and/or -polymeric coordination compounds. These include the bonding modes $\mu_{1,3}\text{-NCS}^-$ [1,5–7,10,21–31], $\mu_{1,1}\text{-NCS}^-$ [32–34], $\mu_{3,3}\text{-NCS}^-$ [35–37], $\mu_{1,1,3}\text{-NCS}^-$ [38], $\mu_{1,3,3}\text{-NCS}^-$ [39], and $\mu_{1,3,3,3}\text{-NCS}^-$ [40]. In compounds where the coordinated isothiocyanate ion is acting as a terminal ligand, then according to Hard Soft Acid Base (HSAB) concept, soft Lewis acid metal ions prefer the soft Lewis S-site and hard metals prefer the soft site [41]. Interestingly, although nitrogen in NCS^- is classified as borderline Lewis base, most hard metals such as Fe^{2+} , Ni^{2+} , Cu^{2+} , Co^{2+} , and Zn^{2+} show high preference to the N-site [42,43].

Herein, we report the synthesis and structural characterization of a series of Cu(II)-isothiocyanato coordination compounds derived from sterically hindered N-donor diamines with different alkyl substituents as co-ligands: the coordination 1D-polymers: *catena*-[Cu(Me₃en)(μ -NCS)(NCS)] (1), *catena*-[Cu(NEt₂Meen)(μ -NCS)(NCS)] (2), *catena*-[Cu(N,N,2,2-Me₄pn)(μ -NCS)(NCS)] (3), the dimeric [Cu₂(N,N'-isp₂en)₂(μ -NCS)₂(NCS)₂] (4), and the monomeric compound [Cu(N,N'-*t*-Bu₂en)(NCS)₂] (5). This should allow us to evaluate the role of the steric effect imposed by the coordinated amine co-ligands in adapting a specific NCS-bonding mode as well as the selected dimensionality. The structures of the ligands used in this study together with other related diamine derivatives are illustrated in Scheme 1. The Density Functional Theory (DFT) computations were performed in an attempt to account for the observed geometrical and dimensionality of 4 and 5 compounds.



Scheme 1. Structures of the ligands used in this study together with other related compounds.

2. Results and Discussion

2.1. Synthetic Aspects

The isolated coordination compounds: *catena*-[Cu(Me₃en)(μ -NCS)(NCS)] (1), *catena*-[Cu(NEt₂Meen)(μ -NCS)(NCS)] (2), *catena*-[Cu(N,N,2,2-Me₄pn)(μ -NCS)(NCS)] (3), [Cu₂(N,N'-isp₂en)₂(μ -NCS)₂(NCS)₂] (4), and [Cu(N,N'-*t*-Bu₂en)(NCS)₂] (5) were synthesized in reasonably good yields (71%–92%) by the reaction of a methanolic solution containing equimolar amounts of Cu(NO₃)₂·3H₂O or Cu(ClO₄)₂·6H₂O and the corresponding diamine ligand with four equivalents of NH₄NCS solution dissolved in H₂O or MeOH. Crystals suitable for X-ray analysis were obtained from dilute solutions or by recrystallization from CH₃CN or anhydrous MeOH. The purity of the coordination compounds was confirmed by elemental microanalyses (see experimental section). Molar conductivities, Λ_M measured in CH₃CN, are within the range of 7–12 $\Omega^{-1}\text{cm}^2\text{mol}^{-1}$ which reflect their non-electrolytic nature [44]. The coordination compounds were also characterized by IR, UV–Vis, and by single crystal X-ray

crystallography. Probably, it is interesting to mention that although the μ -1,3- and μ -1,1-bonding modes are common in bridging-azido-metal(II) coordination compounds [8,9,11,12,14–16], the corresponding μ -1,1-bonding in the bridging-isothiocyanato compounds is rare [32–34] and in most cases alternating μ -1,3-bonding chains are observed [1–7,17,21–31].

2.2. IR and UV–VIS Spectra of the Coordination Compounds

The IR asymmetric stretching frequencies of the isothiocyanato-Cu(II) coordination compounds under investigation and their corresponding UV-Vis spectra in acetonitrile solution are collated in Table 1. It has been stated that the $\nu_{\text{as}}(\text{C}\equiv\text{N})$ frequencies could be used as a criterion to differentiate between the terminally *N*-bonded isothiocyanato anions which in most cases display a value below 2100 cm^{-1} , whereas in the corresponding *S*-bonded and/or μ -1,3-bridging isothiocyanato anions, the stretching vibrations are observed above 2100 cm^{-1} [12,28–31,42,43,45]. The IR spectra of the compounds 1–4 display very strong bands over the $2095\text{--}2131\text{ cm}^{-1}$ region due to $\nu_{\text{as}}(\text{C}\equiv\text{N})$ of the bridged-isothiocyanato ligands. In addition, the same series of coordination compounds as well as 5 showed a strong to medium intensity band over the $2059\text{--}3086\text{ cm}^{-1}$ region which can be attributed to the *N*-bonded terminal isothiocyanate ligand(s). This data are fully consistent with *N*-bonded isothiocyanate in all coordination compounds and μ -1,3-bridging isothiocyanate in 1–4. These were also confirmed by X-ray structural analysis (Section 2.3).

Table 1. The IR asymmetric stretching frequency of the coordinated isothiocyanato groups and UV-Vis spectra of the coordination compounds 1–5 in CH_3CN solution.

Coordination Compound	$\nu_{\text{as}}(\text{C}\equiv\text{N})$ (cm^{-1})	λ_{max} , nm (ϵ , $\text{M}^{-1}\text{cm}^{-1}$)
<i>catena</i> -[Cu(Me ₃ en)(μ -NCS)(NCS)] (1)	2131 (vs), 2086 (vs)	615 (153), 974 (59)
<i>catena</i> -[Cu(NEt ₂ Meen)(μ -NCS)(NCS)] (2)	2095 (vs), 2025 (m)	655 (159)
<i>catena</i> -[Cu(<i>N,N</i> ,2,2-Me ₄ pn)(μ -NCS)(NCS)] (3)	2099 (vs), 2068 (vs)	~656 (136)
[Cu ₂ (<i>N,N'</i> -isp ₂ en) ₂ (μ -NCS) ₂ (NCS) ₂] (4)	2128 (s), 2073 (vs)	~655 (120)
[Cu(<i>N,N'</i> - <i>t</i> -Bu ₂ en)(NCS) ₂] (5)	2059 (vs)	~766 (266), 469 (2160), 299 (3090)

Inspection of the acetonitrile solutions of the UV–Vis spectral data of the coordination compounds 1–4, shown in Table 1, reveals some common spectral features as they display broad maxima in the 615–656 nm region. This feature is consistent with five-coordinate Cu(II) compounds with square pyramidal geometry (SP) which may be associated with a low-energy shoulder at $\lambda > 800\text{ nm}$ [28–31,42,43,45–50]. The presence of the small intense maxima at 974 nm in compound 1 may reflect the increased distortion towards the trigonal bipyramidal geometry (TBP) [45]. Obviously, compound 4 does not belong to the observed geometry but instead it has one visible maxima at ~766 nm, resulting from *d*–*d* transition; $^2\text{E} \leftarrow ^2\text{T}$ in tetrahedral environment [51]. The very strong intense band located at 469 nm can be assigned to ligand–metal charge transfer transition (*L*→*M* CT), whereas the 299 nm maxima is most likely attributable to electronic transition within the NCS^- ligand ($\pi \rightarrow \pi^*$). The solid spectra of complexes 1–4 showed a similar spectral pattern with two maxima located at 480–520 and 630–690 nm regions and a shoulder around 730–750 nm (Figures S1–S4 in the Supplementary Materials for 1–4 compounds, respectively). The geometrical finding around the Cu(II) ion in acetonitrile solution was retained in the solid state as it was supported by the X-ray structural data.

2.3. Description of the Structures

2.3.1. *catena*-[Cu(Me₃en)(μ -NCS)(NCS)] (1), *catena*-[Cu(NEt₂Meen)(μ -NCS)(NCS)] (2), and *catena*-[Cu(*N,N*,2,2-Me₄pn)(μ -NCS)(NCS)] (3)

Perspective views with the atom numbering scheme for the polymeric coordination compounds 1–3 are presented in Figures 1–3 and Tables S1–S3 summarize main bond parameters. The copper(II) centers are linked by single μ _{1,3}-isothiocyanato bridges to form polymeric chains of polyhedra (1D).

Each metal center is *penta*-coordinated by two *N*-donor atoms of the amine ligand and two *N*-atoms of terminal and bridging *N,S*-NCS[−] anions (atoms with minor split occupancy in partially disordered crystal structure of compound **1** were ignored). The CuN₄S chromophores may be described as distorted SP geometry. The basal Cu–N bond distances are in the range of 1.9487(13) to 2.106(7) Å. The S-atoms of the bridging NCS[−] groups are located in apical positions [Cu–S from 2.6421(11) to 2.8910(16)]. The Cu⋯Cu' distances within the chain are 5.4245(11), 5.7755(9), and 5.7679(15) Å, for **1–3**, respectively. The shortest metal–metal separations between the chains are 6.7646(16), 6.8602(10), and 6.9132(16) Å, for **1–3**, respectively. Hydrogen bonds of type N–H⋯S are formed between *N*-amine ligand to S atoms of neighboring Cu(II)-polyhedra (Table 2, Figures S5–S7) to form a supramolecular 2D system in case of **1** and **3**, respectively.

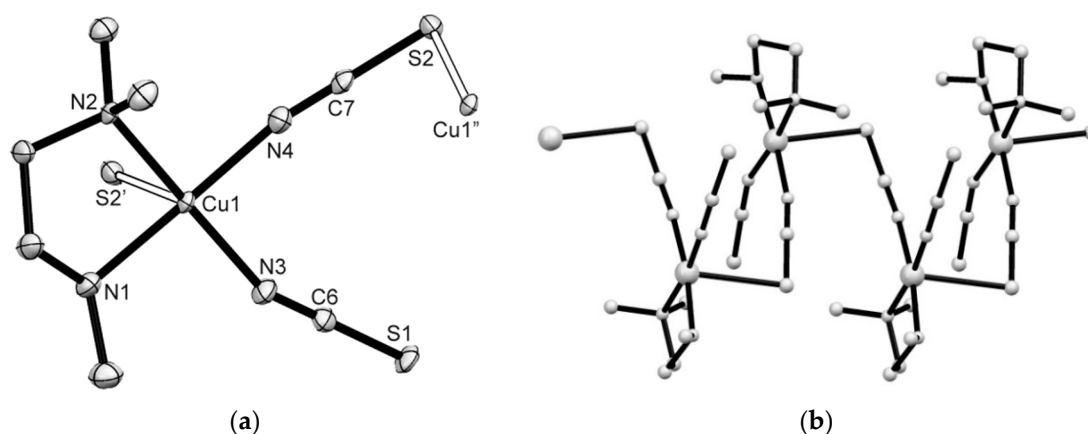


Figure 1. (a) Perspective view of the asymmetric unit and the Cu(II) coordination core of **1** (50% probability ellipsoids, only the major disorder form given for clarity). Symmetry codes: (') $3/2-x, 1-y, 1/2+z$; (") $3/2-x, 1-y, -1/2+z$. Selected bond distances (Å) and angles (°): Cu(1)–N(4) 1.952(4), Cu(1)–N(3) 1.966(4), Cu(1)–N(1) 2.024(4), Cu(1)–N(2) 2.066(3), Cu(1)–S(2') 2.8910(16); N(4)–Cu(1)–N(1) 172.27(19), N(3)–Cu(1)–N(2) 171.9(2). (b) View of a section of the polymeric chain of **1**.

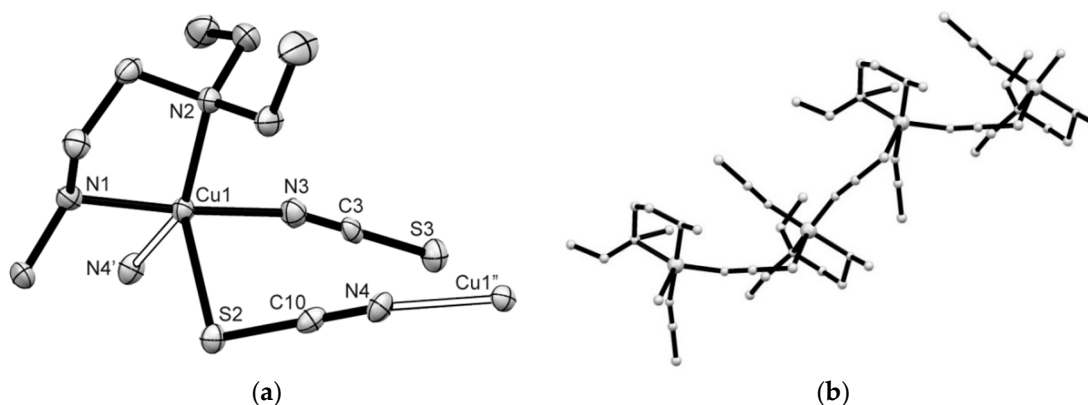


Figure 2. (a) Perspective view of the asymmetric unit and the Cu(II) coordination core of **2** (50% probability ellipsoids). Symmetry codes: (') $x, 1/2-y, -1/2+z$; (") $x, 1/2-y, 1/2+z$. Selected bond distances (Å) and angles (°): Cu(1)–N(3) 1.957(3), Cu(1)–N(4') 1.992(3), Cu(1)–N(1) 2.009(3), Cu(1)–N(2) 2.094(3), Cu(1)–S(2) 2.6421(11); N(4)–Cu(1)–N(1) 172.27(19), N(3)–Cu(1)–N(2) 171.9(2). (b) View of a section of the polymeric chain of **2**.

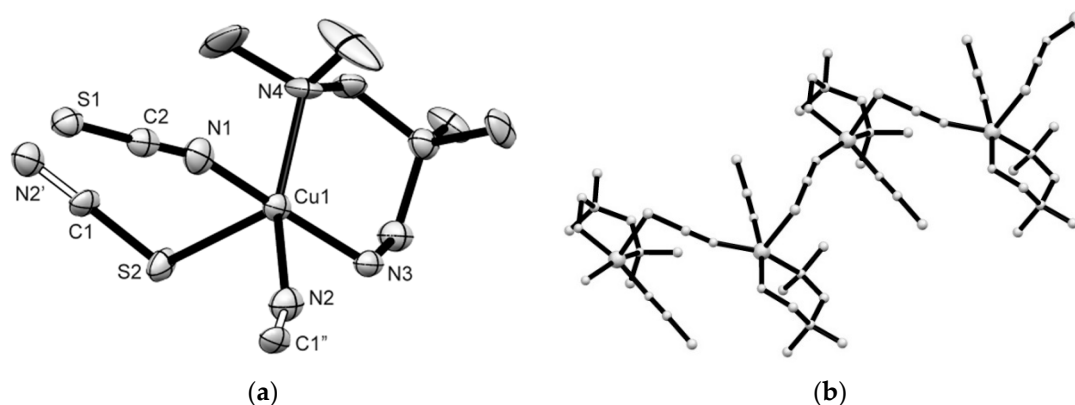


Figure 3. (a) Perspective view of the asymmetric unit and the Cu(II) coordination core of **3** (50% probability ellipsoids). Symmetry codes: (') $x, 1/2-y, 1/2+z$; (") $x, 1/2-y, -1/2+z$. Selected bond distances (Å) and angles ($^{\circ}$): Cu(1)-N(1) 1.955(6), Cu(1)-N(3) 1.987(5), Cu(1)-N(2) 2.024(5), Cu(1)-N(4) 2.112(5), Cu(1)-S(2) 2.6183(16); N(3)-Cu(1)-N(1) 170.08(19), N(4)-Cu(1)-N(2) 157.0(2). (b) View of a section of the polymeric chain of **3**.

Table 2. Possible hydrogen bonds in crystal structures 1–5.

D–H ... A ^a	Symmetry of A	D–H (Å)	D ... A (Å)	D–H...A ($^{\circ}$)
Compound 1				
N(1)–H(1) ... S(1)	$1/2+x, 1/2-y, 1-z$	0.91(3)	3.446(4)	147(5)
Compound 2				
N(1)–H(90) ... S(3)	$x, 1/2-y, -1/2+z$	0.82(4)	3.519(3)	158(4)
Compound 3				
N(3)–H(3A) ... S(1)	$x, 1/2-y, -1/2+z$	1.00(7)	3.575(4)	173(4)
N(3)–H(3B) ... S(1)	$2-x, -1/2+y, 1/2-z$	0.90(6)	3.483(5)	170(5)
Compound 4				
N(3)–H(31) ... S(1)	$x, 1/2-y, 1/2+z$	0.85(2)	3.4711(13)	157(2)
Compound 5				
N(3)–H(31) ... S(1)	$2-x, -y, -z$	0.77(2)	3.3943(17)	173(2)
N(4)–H(41) ... S(1)	$x, 1/2-y, 1/2+z$	0.80(2)	3.4710(17)	171(2)

^a D = donor, A = acceptor.

2.3.2. $[\text{Cu}_2(\text{N},\text{N}'\text{-isp}_2\text{en})_2(\mu\text{-NCS})_2(\text{NCS})_2]$ (**4**)

Compound **4** consists of centrosymmetric dimeric $[\text{Cu}_2(\text{N},\text{N}'\text{-isp}_2\text{en})_2(\mu\text{-NCS})_2(\text{NCS})_2]$ units (Figure 4). Each Cu(II) center is *penta*-coordinated by two N-atoms of *N,N'*-isp₂en ligand, two N-atoms of terminal and bridging NCS[−] anions and an S-atom of the bridging NCS[−] anion. The CuN₄S chromophore is described as a distorted polyhedron with intermediate geometry between SP and TBP and a τ value of 0.50. The apical site is occupied by the S(1') atom [Cu(1)–S(1') = 2.9037(6) Å]. The basal Cu–N bonds vary from 1.9487(13) to 2.0388(12) Å. The $\mu_{1,3}$ -isothiocyanato bridges connect two Cu(II) polyhedron to centrosymmetric dimeric units. Their eight-membered Cu(NCS)₂Cu rings are almost planar ("chair angle" θ which is defined as acute angle between plane of the di- $\mu_{1,3}$ -isothiocyanato bridges and the Cu/N(1)/S(1) plane is 2.5 $^{\circ}$). The Cu(1) ... Cu(1') distance within the Cu(NCS)₂Cu ring is 5.8794(8) Å, and the inter-dimer separation is 6.6979(9) Å. The Cu–N ... S–Cu' torsion angle is 23.2 $^{\circ}$, the Cu–N–C–S torsion angles are −139.4 and 87.9 $^{\circ}$. Hydrogen bonds of type N–H ... S are formed between N(3) atoms of *N,N'*-isp₂en ligand to the S(1) atom of neighboring Cu-polyhedra to generate a supramolecular 2D system oriented along the *b*- and *c*-axis of the unit cell (Table 2, Figure S8).

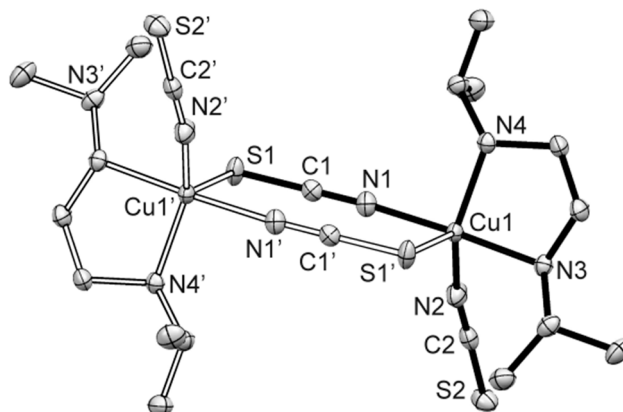


Figure 4. Perspective view of the dimeric compound **4** (60% probability ellipsoids). Symmetry code: (') $2-x, -y, -z$. Selected bond distances (Å) and angles ($^{\circ}$): Cu(1)–N(1) 1.9487(13), Cu(1)–N(2) 1.9712(12), Cu(1)–N(3) 2.0312(12), Cu(1)–N(4) 2.0386(12), Cu(1)–S(1') 2.9037(6); N(3)–Cu(1)–N(1) 173.67(5), N(4)–Cu(1)–N(2) 143.78(5).

2.3.3. $[\text{Cu}(\text{N},\text{N}'\text{-}t\text{-Bu}_2\text{en})(\text{NCS})_2]$ (**5**)

Compound **5** consists of monomeric neutral $[\text{Cu}(\text{N},\text{N}'\text{-}t\text{-Bu}_2\text{en})(\text{NCS})_2]$ units where the Cu(II) centers are tetrahedrally coordinated by four nitrogen donor atoms: two belong to the $\text{N},\text{N}'\text{-}t\text{-Bu}_2\text{en}$ ligand and two belong to N -terminal isothiocyanato anions (Figure 5). The Cu–N bond distances are in the range from 1.9299(17) to 2.0108(16) Å. The distorted coordination tetrahedra form N–Cu–N bond angles in the range from 97.03(7) to 140.14(7) $^{\circ}$. The shortest Cu...Cu separation is 6.4592(9) Å. Hydrogen bonds of type N–H...S are formed between N(3) and N(4) atoms of $\text{N},\text{N}'\text{-}t\text{-Bu}_2\text{en}$ ligand to S(1) atoms of neighboring Cu-polyhedra to generate a supramolecular 2D system oriented along the b - and c -axis of the unit cell (Table 2, Figure S9).

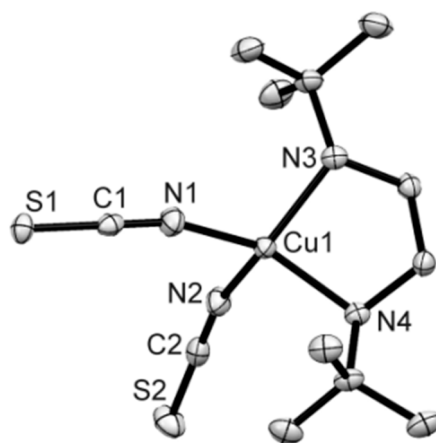


Figure 5. Molecular plot of **5** (50% probability ellipsoids). Selected bond distances (Å) and angles ($^{\circ}$): Cu(1)–N(1) 1.9378(17), Cu(1)–N(2) 1.9303(17), Cu(1)–N(3) 2.0102(16), Cu(1)–N(4) 2.0037(16); N(1)–Cu(1)–N(4) 140.11(7), N(3)–Cu(1)–N(2) 138.29(7).

We think it would be interesting to compare our structural results of compounds **1–5** with the literature data of Cu(II)-isothiocyanato coordination compounds which are derived from related bidentate amines and these compounds together with ours are collated in Table 3. Inspection of this data may show some general trends about the coordination behavior of these compounds. The isothiocyanato compounds which are constructed from ethylenediamine (en) [52–56], mono- N -alkyl ethylenediamine (Me-en, propen) [57,58], less hindered di(N,N' -alkyl)-ethylenediamine ($\text{N},\text{N}'\text{-Me}_2\text{en}$) [59] and 1,5-diazacyclooctane (DACO) [60] resulted in the formation of mono-nuclear Cu(II)-bis(diamine) compounds with or without N -NCS-coordination. With very bulky di(N,N' -alkyl)-ethylenediamine;

N,N' -*t*-Bu₂en, only mono-nuclear Cu(II)-(diamine), [Cu(N,N' -*t*-Bu₂en)(NCS)₂] (**5**) was formed with *N*-NCS-coordination. However, when one of the methyl groups in each of the *tert*-butyl moieties in N,N' -*t*-Bu₂en was replaced by hydrogen in order to moderate and relieve the steric environment (N,N' -isp₂en), the dinuclear bridged-NCS coordination compound [Cu₂(N,N' -isp₂en)₂(μ₂-NCS)₂(NCS)₂] (**4**) was isolated. On the other hand, the isothiocyanato coordination compounds which were constructed from *N,N*-dialkyl, *N,N,N'*-trialkyl- and/or tetra-*N,N,N',N'*-tetraalkyl-diamine ligands afforded five-coordinate 1D-polymeric chains, where the Cu(II)-(diamine) moieties are μ_{N,S}-NCS bridged and the coordination geometry is achieved by another *N*-NCS group [61–64] as this was the case observed in the 1–3 compounds under investigation.

Table 3. Some structural details of Cu(II)-isothiocyanate coordination compounds derived from some *N*-alkyl bidentate amine ligands. ^a

Compound	C.N.; Nuc. ^b	NCS-Bonding	Refcode [Ref]
[Cu(en) ₂]Br(NCS)	4; mono	non-coord.	BITJIX [52]
[Cu(en) ₂](NCS)(ClO ₄)	4; mono	non-coord.	ENCUTP [53]
[Cu(en) ₂](NCS) ₂	4; mono	non-coord.	EDCOPT [54]
[Cu(en) ₂](NCS)(BF ₄)	4; mono	non-coord.	GASRUN [55]
[Cu(en) ₂](NCS) ₂	4; mono	non-coord.	TCENCU [56]
[Cu(en)(NCS) ₂ (H ₂ O)]	5; mono	<i>N</i> -NCS	HIQGUJ [65]
[Cu(Me-en) ₂ (NCS)](NCS)	5; mono	<i>N</i> -NCS, non-coord.	MEENCU [66]
[Cu(N,N' -Me ₂ en) ₂](NCS) ₂	4; mono	non-coord.	MENCUT [59]
[Cu(propen) ₂](NCS) ₂	4; mono	non-coord.	APRCUT [57]
[Cu(propen) ₂ (NCS)]ClO ₄	5; mono	<i>N</i> -NCS	DAPICU [58]
[Cu(DACO) ₂ (NCS)](NCS)(H ₂ O)	5; mono	<i>N</i> -NCS, non-coord.	FEKHAF [60]
[Cu(N,N' - <i>t</i> -Bu ₂ en)(NCS) ₂] (5)	4; mono	<i>N</i> -NCS	This work
[Cu ₂ (N,N' -isp ₂ en) ₂ (μ ₂ -NCS) ₂ (NCS) ₂] (4)	5, dimer	di-μ _{N,S} , <i>N</i> -NCS	This work
<i>catena</i> -[Cu(NEt ₂ en)(μ-NCS)(NCS)]	5, 1D	μ _{N,S} , <i>N</i> -NCS	XIBXAI [61]
<i>catena</i> -[Cu(Me ₄ en)(μ-NCS)(NCS)]	5; 1D	μ _{N,S} , <i>N</i> -NCS	DUBNIZ [62]
<i>catena</i> -[Cu(Me ₃ en)(μ-NCS)(NCS)] (1)	5, 1D	μ _{N,S} , <i>N</i> -NCS	This work
<i>catena</i> -[Cu(NEt ₂ Meen)(μ-NCS)(NCS)] (2)	5, 1D	μ _{N,S} , <i>N</i> -NCS	This work
<i>catena</i> -[Cu(NMe ₂ propen)(μ-NCS)(NCS)]	5; 1D	μ _{N,S} , <i>N</i> -NCS	SEZFAF [63]
<i>catena</i> -[Cu($N,N,2,2$ -Me ₄ pn)(μ-NCS)(NCS)] (3)	5, 1D	μ _{N,S} , <i>N</i> -NCS	This work
<i>catena</i> -[Cu(DACO)(μ-NCS)(NCS)]	5; 1D	μ _{N,S} , <i>N</i> -NCS	FODQOF [64]

^a Structures of the ligands and their abbreviations are shown in shown in Scheme 1. ^b C.N. = coordination number of Cu(II) and Nuc = nuclearity.

2.4. The DFT Computational Results

DFT was used in order to garner insights into the aggregation properties of the various Cu coordination compounds. In particular, we were interested in the intrinsic reasons for the ligand specific variations in adapting a certain mono- or polynuclear chain size. Figure 6 shows the geometries and energetics associated with various oligomeric arrangements of **5** and **4**. Figure 6a shows the ground state minimum energy geometry of Cu(I), Cu(II), and Cu(III) oxidation states of monomeric **5**; The N,N' -*t*-Bu₂en ligand tends to form a mononuclear tetrahedral arrangement around the metal center which is in good agreement with the X-ray crystal structure results. The Cu(I) the lowest energy charge of **5** is -1 , which can be understood by considering that the entire coordination compound is closed-shell when Cu is in the $+1$ oxidation state. Attempts were made to dimerize **5** with overall charges of neutral, $+1$ and -1 . Upon optimization, the neutral coordination compound associates and forms a stable dimer, the $+1$ and -1 charged **5** dimers dissociate and form a monomer pair at an asymptotic separation. The neutral compound forms a stable dimer but it is at a higher energy state when compared to the -1 coordination compound of **5**. Thus, the Cu(I) coordination compound **5** is the lowest energy oxidation state of the metal-center and yields a coordination compound with an overall charge of -1 ; The -1 charge of **5** leads to prompt dissociation of a dimer upon geometry optimization—forming two monomers.

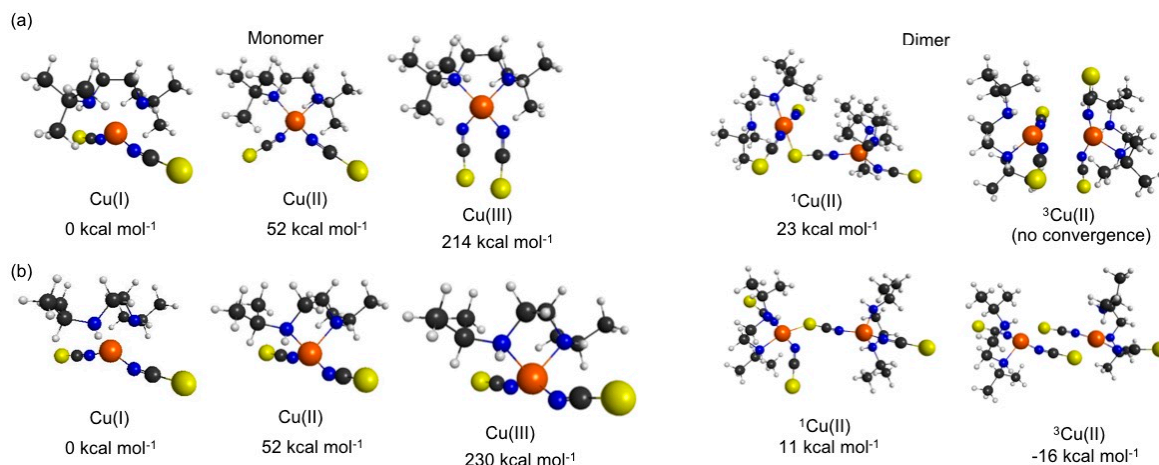


Figure 6. Geometries associated with the ground state minima of (a) **5** and (b) **4**. The dimer geometries are relative to the energy of the Cu(I) + Cu(I) monomer asymptote at infinite separation.

Analogous computations on **4** also returned Cu(I) as the lowest energy oxidation state of the metal-center. Attempts to dimerize **4** were successful for the lowest energy triplet state of Cu(II) (henceforth ³Cu(II)) oxidation state and, unlike **5**, did not dissociate to form two monomers upon optimization. The dimer form of triplet-Cu(II) of **4** is lower than the monomer forms by ~16 kcal/mol. All other oxidation states of Cu of **4** failed to converge to a dimer and yielded two monomers. However, further attempts to trimerize **4** were unsuccessful and yielded a dimer + monomer at an infinite separation upon optimization. This observation is again in line with the observed dimeric crystal structure of **4**.

In comparing **5** with **4**, we postulate that the bulky *tert*-butyl moiety in **5** shows an enhanced steric hindrance, thus inhibiting its ability to sustain a polymeric structure. The loss of two methyl groups in **5** leads to some reduction in such steric hindrance. As a result, **4** is able to sustain a dimeric crystal structure but unable to maintain a larger oligomeric arrangement since (en)₂ remains a bulky group that introduces steric hindrance. With the available resources and large molecular sizes, coordination compounds **1**, **2**, and **3** produced computationally challenging structures. However, using the available computational data for **5** and **4** we were able to postulate that similar steric arguments would hold in the cases of **1–3** since the bulky *N*-alkyl substituents at the ethylenediamine co-ligand becomes progressively less favorable across this series.

3. Experimental Section

3.1. Materials and Physical Measurements

N,N,N'-Trimethylethylenediamine (Me₃en), *N,N*-diethyl-*N'*-methylethylenediamine (Et₂Meen), *N,N,2,2*-tetramethylpropylenediamine (*N,N,2,2*-Me₄pn), *N,N'*-diisopropylethylenediamine (*N,N'*-isp₂en), and *N,N'*-di(*tert*-butyl)ethylenediamine (*N,N'*-*t*-Bu₂en) were purchased from TCI-America. All other commercially available chemicals were used without further purification. Infrared spectra of solid samples were measured on a Cary 630 (FT IR-ATR) spectrometer. Electronic spectra in acetonitrile were measured using an Agilent 8453 HP diode array UV-Vis spectrophotometer, whereas the corresponding solid spectra of **1–4** compounds were performed with an LS 950 Perkin-Elmer Lambda-spectrometer in the 350–950 nm range. A Mettler Toledo Seven Easy conductivity meter was used for conductivity measurements. For its calibration a 1413 μS/cm conductivity standard was used. Elemental analyses were performed by the Atlantic Microlaboratory, Norcross, Georgia, USA.

3.2. Syntheses of the Coordination Compounds

Catena-[Cu(Me₃en)(μ-NCS)(NCS)] (1). A mixture of Cu(ClO₄)₂·6H₂O (0.186 g, 0.5 mmol), *N,N,N'*-trimethylethylenediamine (Me₃en) (0.051 g, 0.50 mmol), and NH₄NCS (0.152 g, 2.0 mmol) was dissolved in MeOH (20 mL) and the resulting dark green solution was heated for 5 min, filtered while hot, and allowed to stand at room temperature. The precipitate obtained after 2 h was collected and crystallized from CH₃CN to afford navy blue single crystals. These were collected by filtration, washed with propan-2-ol, Et₂O, and air dried (yield: 0.105 g, 74%). Anal. Calcd for C₇H₁₄CuN₄S₂ (MM = 281.89 g/mol): C, 29.83, H, 5.01, N, 19.88%. Found: C, 29.92, H, 4.86, N, 19.92%. Selected IR bands (ATR-IR, cm⁻¹): 3178 (w) (N-H stretching), 2921 (w) (aliphatic C-H stretching), 2131 (vs), 2086 (vs) (C≡N stretching of NCS⁻). UV-Vis spectrum {λ_{max}, nm (ε, M⁻¹cm⁻¹)} in CH₃CN: 615 (153), 974 (59). Λ_M (CH₃CN) = 8 Ω⁻¹cm²mol⁻¹.

Catena-[Cu(Et₂Meen)(μ-NCS)(NCS)] (2). To a mixture containing Cu(NO₃)₂·3H₂O (0.241g, 1.0 mmol), *N,N*-diethyl-*N'*-methylethylenediamine (Et₂Meen) (0.130 g, 1.0 mmol) dissolved in MeOH (25 mL), an aqueous solution of NH₄NCS (0.152 g, 2.0 mmol dissolved in 5 mL H₂O) was added drop by drop and the reaction mixture was heated for 5 min, filtered through celite and then allowed to crystallize at room temperature. The green precipitate which separated was recrystallized from anhydrous MeOH and the resulting long needle crystals were collected by filtration, washed with propan-2-ol, Et₂O, and air dried (yield: 0.227 g, 73%). Anal. Calcd for C₉H₁₈CuN₄S₂ (MM = 309.94 g/mol): C, 34.88; H, 5.85; N, 18.08%. Found: C, 35.02, H, 5.97, N, 17.89%. Selected IR bands (ATR-IR, cm⁻¹): 3168 (w) (N-H stretching), 2974 (w), 2933 (vw), 2878 (vw) (aliphatic C-H stretching), 2095 (vs) (C≡N stretching of NCS⁻). UV-Vis spectrum {λ_{max}, nm (ε, M⁻¹cm⁻¹)} in CH₃CN: 655 (159). Λ_M (CH₃CN) = 11 Ω⁻¹cm²mol⁻¹.

Catena-[Cu(N,N,2,2-Me₄pn)(μ-NCS)(NCS)] (3). This compound was isolated as green single crystals and prepared using a similar procedure to that described for **2**, except *N,N,2,2*-tetramethylpropylenediamine was used instead of Et₂Meen (yield: 92%). Anal. Calcd for C₉H₁₈CuN₄S₂ (MM = 309.94 g/mol): C, 34.88; H, 5.85; N, 18.08%. Found: C, 34.67; H, 5.55; N, 18.30%. Selected IR bands (ATR-IR, cm⁻¹): 3291 (w), 3225 (N-H stretching), 2995 (vw), 2965 (w), 2886 (vw), 2842 (vw) (aliphatic C-H stretching), 2099 (vs), 2068 (vs) (C≡N stretching of NCS⁻). UV-Vis spectrum {λ_{max}, nm (ε, M⁻¹cm⁻¹)} in CH₃CN: ~656 (136). Λ_M (CH₃CN) = 12 Ω⁻¹cm²mol⁻¹.

[Cu₂(N,N'-isp₂en)₂(μ₂-NCS)₂(NCS)₂] (4). Green single crystals were obtained from a methanolic solution using a procedure similar to that described for **2**, with *N,N'*-diisopropylethylenediamine (*N,N'*-isp₂en) used instead of Et₂Meen (yield: 79%). Anal. Calcd for C₂₀H₄₀Cu₂N₈S₄ (MM = 647.94 g/mol): C, 37.08; H, 6.22; N, 17.29%. Found: C, 36.80; H, 6.06; N, 17.25%. Selected IR bands (ATR-IR, cm⁻¹): 3213 (w), 3158 (w) (N-H stretching), 2975 (w), 2964 (vw), 2925 (vw), 2876 (vw) (aliphatic C-H stretching), 2128 (s), 2073 (vs) (C≡N stretching of NCS⁻). UV-Vis spectrum {λ_{max}, nm (ε, M⁻¹cm⁻¹)} in CH₃CN: ~655 (120). Λ_M (CH₃CN) = 12 Ω⁻¹cm²mol⁻¹.

[Cu(N,N'-t-Bu₂en)(NCS)₂] (5). Green single crystals were separated from a methanolic solution using a procedure similar to that described for **2**, with *N,N'*-di(*tert*-butyl)ethylenediamine (*N,N'*-*t*-Bu₂en) used instead of Et₂Meen (yield: 71%). Anal. Calcd for C₁₂H₂₄CuN₄S₂ (MM = 352.02 g/mol): C, 40.94; H, 6.87; N, 15.92%. Found: C, 41.08; H, 6.72; N, 16.21%. %. Selected IR bands (ATR-IR, cm⁻¹): 3242 (m) (N-H stretching), 2972 (w), 2859 (vw) (aliphatic C-H stretching), 2059 (vs) (C≡N stretching of NCS⁻). UV-Vis spectrum {λ_{max}, nm (ε, M⁻¹cm⁻¹)} in CH₃CN: ~766 (266), 469 (2160), 299 (3090). Λ_M (CH₃CN) = 7 Ω⁻¹cm²mol⁻¹.

3.3. X-ray Crystal Structure Analysis and Refinement

A Bruker-AXS APEX II CCD diffractometer operating at 100(2) K was used for single-crystal X-ray measurements of compounds **1**–**5**. Tables 4 and 5 summarize the crystallographic data, parameters for intensity data collection and structure refinement. Mo-Kα radiation (λ = 0.71073 Å) was used for

data collection. The computer programs SAINT (Version 7. 23; Bruker AXS Inc.: Madison, WI, USA, 2005), APEX (Version 2. 0-2; Bruker AXS Inc.: Madison, WI, USA, 2006), and SADABS [67] were used for data processing, and corrections for Lorentz-Polarisation and absorption effects. The SHELXTL program package [68] with implemented direct methods as well as full-matrix least-squares refinement procedures operating on F^2 was used for structure solutions and refinements. Anisotropic displacement parameters were applied to non-hydrogen atoms. The positions of hydrogen atoms were taken from difference Fourier maps and their isotropic displacement factors U_{iso} set to 1.2 to 1.5 times U_{eq} of parent C or N atom. Geometrical constraints (HFIX) were applied for H atoms bonded to C atoms. The MERCURY program [69] was used to perform molecular plots. In compound **1**, the central Cu atom and the S atom of the terminal isothiocyanate group are disordered over two positions and refined with 90/10 split occupancy using free variables to refine the respective occupancy of the affected fragment (PART) [70]. ISOR and EADP were applied to the disordered atoms to make ADP values for these atoms more reasonable. In compound **1**, the N1–H1 distance in the Me₃en donor was restrained using DFIX 0.87 0.02, whereas structure refinements of **2–5** were performed without any restraints for H atoms involved in hydrogen bonds. Compound **1** was refined as a 2-component inversion twin (-100 0-10 00-1) using the TWIN option in SHELXL resulting in BASF = 0.33. Deposition numbers: CCDC 1878247-1878251 for **1–5**, respectively.

Table 4. Crystallographic data and processing parameters for **1–3**.

Compound	1	2	3
Empirical formula	C ₇ H ₁₄ CuN ₄ S ₂	C ₉ H ₁₈ CuN ₄ S ₂	C ₉ H ₁₈ CuN ₄ S ₂
Formula mass	281.89	309.94	309.94
System	Orthorhombic	Monoclinic	Monoclinic
Space group	P2 ₁ 2 ₁ 2 ₁	P2 ₁ /c	P2 ₁ /c
a (Å)	10.9708(6)	12.5637(13)	10.2410(11)
b (Å)	15.6954(9)	10.6338(11)	13.1290(14)
c (Å)	6.7646(4)	10.9288(12)	10.2040(11)
α (°)	90	90	90
β (°)	90	105.709(13)	92.308(19)
γ (°)	90	90	90
V (Å ³)	1164.80(12)	1405.6(3)	1370.9(3)
Z	4	4	4
T (K)	100(2)	100(2)	100(2)
μ (mm ⁻¹)	2.202	1.832	1.878
D _{calc} (Mg/m ³)	1.607	1.465	1.502
Crystal size (mm)	0.09 × 0.07 × 0.05	0.40 × 0.08 × 0.04	0.22 × 0.10 × 0.08
θ max (°)	33.207	26.332	25.998
Data collected	48,125	10,871	10,458
Unique refl./R _{int}	4443/0.1330	2860/0.0587	2696/0.0799
Parameters/restraints	142/13	151/0	155/0
Goodness-of-Fit on F ²	1.049	1.065	1.068
R1/wR2 (all data)	0.0502/0.1157	0.0497/0.1089	0.0660/0.1623
Residual extrema (e/Å ³)	1.61/−0.77	0.73/−0.50	1.27/−0.50

Table 5. Crystallographic data and processing parameters for **4** and **5**.

Compound	4	5
Empirical formula	C ₂₀ H ₄₀ Cu ₂ N ₈ S ₄	C ₁₂ H ₂₄ CuN ₄ S ₂
Formula mass	647.94	352.02
System	Monoclinic	Monoclinic
Space group	P2 ₁ /c	P2 ₁ /c
a (Å)	8.3074(10)	9.0079(11)
b (Å)	12.4648(13)	13.2386(13)
c (Å)	14.4011(15)	14.7134(14)
α (°)	90	90
β (°)	106.187(3)	103.156(3)
γ (°)	90	90
V (Å ³)	1432.1(3)	1708.6(3)
Z	2	4
T (K)	100(2)	100(2)
μ (mm ⁻¹)	1.802	1.516
D _{calc} (Mg/m ³)	1.503	1.368
Crystal size (mm)	0.30 × 0.18 × 0.13	0.33 × 0.22 × 0.15
θ max (°)	26.310	26.365
Data collected	11,053	13,358
Unique refl./R _{int}	2894/0.0252	3464/0.0327
Parameters/restraints	164/0	184/0
Goodness-of-Fit on F ²	1.052	1.058
R1/wR2 (all data)	0.0203/0.0535	0.0294/0.0729
Residual extrema (e/Å ³)	0.34/−0.43	0.40/−0.21

3.4. The Computational Methodology

The ground state minimum energy geometry of the various structures was optimized with density functional theory (DFT), using the Becke-3 parameter-Lee-Yang-Parr (B3LYP) functional [71] and the 6-31G(d) Pople basis set [72]. The increasing size and molecular coordination commodity of the oligomeric metal coordination compounds precluded the use of higher levels of theory. The B3LYP/6-31G(d) level is therefore an adequate compromise between accuracy and computational expense and allows for a qualitative comparison between polymers of varying size. The individual Cu-compounds may associate to form oligomers of varying chain length. Association energies were calculated by optimizing a given polymer and their associated monomers and smaller oligomers that make up the polymers. Computations were performed on both Cu(I) and Cu(III) oxidation states in order to determine the dominant oxidation state in a given oligomer. Computations of the normal mode wavenumbers were proved to be computationally too expensive due mostly to the large molecular sizes and the heavy metal effects. The Gaussian 09 computational package was used to perform all computations [73].

4. Conclusions

Five different Cu(II)-isothiocyanate coordination compounds were constructed from *N*-donors bidentate amine ligands including the polymeric 1D-chains *catena*-[Cu(Me₃en)(μ-NCS)(NCS)] (**1**), *catena*-[Cu(NEt₂Meen)(μ-NCS)(NCS)] (**2**), *catena*-[Cu(*N,N*,2,2-Me₄pn)(μ-NCS)(NCS)] (**3**), the dimeric [Cu₂(*N,N'*-isp₂en)₂(μ-NCS)₂(NCS)₂] (**4**), and the monomeric coordination compound [Cu(*N,N'*-*t*-Bu₂en)(NCS)₂] (**5**), where the NCS[−] ions bridge the metal centers in **1–4** with *N*-NCS terminal binding to the Cu²⁺ ion in **5**. The extent of nuclearity (monomer, dimer or polymer) and the isothiocyanate bonding mode (*N*-NCS vs. μ_{*N,S*}-NCS-bridging) depend entirely on the steric hindrance imposed by the *N*-alkyl groups introduced into the *N*-donors amines. In general, when *N,N*-dialkyl, *N,N,N'*-trialkyl- and/or tetra-*N,N,N',N'*-tetraalkyl-diamines were employed as ligands, Cu(II)-(diamine)-(μ₂-NCS)-(N-NCS) 1D-polymeric chains were obtained (**1–3** coordination compounds). With high sterically hindered *N,N'*-dialkyl bidentate amines, only

Cu(II)-(diamine)(*N*-NCS)₂ as was the case in compound **5**, whereas with moderate steric environment such as in *N,N'*-isp₂en, similar species to those **1–3** were produced but with dinuclear composition, [Cu₂(*N,N'*-isp₂en)₂(μ₂-NCS)₂(NCS)₂] (**4**).

Probably, we should mention that geometrical tetrahedral Cu(II) coordination compounds similar to **5** are very rare because the vast majority of Cu(II) compounds display distorted octahedral, trigonal bipyramidal, square pyramidal, and in a few cases square planar geometries. However, monomeric tetrahedral coordination compounds, [Cu(L)₂(NCS)₂] (L = substituted pyridine derivatives) with a composition similar to **5** have been recently reported [74]. In addition, tetrahedral Cu(II) coordination compounds with two bidentate ligands of bis(3,5-dibromo-*N-p*-tolyl-salicylaldiminate) [75], and with a tridentate N₃ ligand and the fourth coordination site occupied with a labile ligand in a C_{3v} symmetry [76] have also been structurally recognized.

Supplementary Materials: The following are available online at <http://www.mdpi.com/2073-4352/9/1/38/s1>. Selected bond lengths (Å) and angles (°) for the compounds under investigation are given in Tables S1–S5 and their corresponding packing views are shown in Figures S5–S9 for **1–5** coordination compounds, respectively. UV–VIS spectra of solid compounds **1–4** are presented as Figures S1–S4, respectively.

Author Contributions: F.A.M., R.C.F. and A.T. performed the X-ray structural analysis. S.S.M., M.M.H., A.M., H.D. and F.R.L. contributed in the synthesis and spectral characterization of the designed compounds. T.N.V.K. performed the computational study. F.A.M., S.S.M., F.R.L. and T.N.V.K. contributed to the writing of the manuscript.

Funding: This research received no external funding.

Acknowledgments: S.S.M. acknowledges the financial support of this research by the Department of Chemistry University of Louisiana at Lafayette. F.A.M. thanks J. Baumgartner (TU Graz) for assistance.

Conflicts of Interest: The authors declare no conflict of interest.

References

1. Shurdha, E.; Moore, C.E.; Rheingold, A.L.; Lapidus, S.H.; Stephens, P.W.; Arif, A.M.; Miller, J.S. First row transition metal(II) thiocyanate coordination compounds, and formation of 1-, 2-, and 3-dimensional extended network structures of M(NCS)₂(solvent)₂ (M = Cr, Mn, Co) composition. *Inorg. Chem.* **2013**, *52*, 10583–10594.
2. Escuera, A.; Estebana, J.; Perlepesb, S.P.; Stamatatos, T.C. The bridging azido as a central “player” in high-nuclearity 3d-metal cluster (M = Cr, Mn, Co) composition. *Coord. Chem. Rev.* **2014**, *275*, 87–129. [[CrossRef](#)]
3. Palion-Gazda, J.; Machura, B.; Lloret, F.; Julve, M. Ferromagnetic coupling through the end-to-end thiocyanate bridge in cobalt(II) and nickel(II) chains. *Cryst. Growth Des.* **2015**, *15*, 2380–2388. [[CrossRef](#)]
4. Żurowska, B.; Mroziński, J.; Julve, M.; Lloret, F.; Maslejova, A.; Sawka-Dobrowolska, W. Structural, spectral, and magnetic properties of end-to-end Di-μ-thiocyanato-bridged polymeric coordination compounds of Ni(II) and Co(II). X-ray crystal structure of di-μ-thiocyanatobis(imidazole)nickel(II). *Inorg. Chem.* **2002**, *41*, 1771–1777. [[CrossRef](#)] [[PubMed](#)]
5. Rams, M.; Tomkowicz, Z.; Runecveski, T.; Böhme, M.; Plass, W.; Suckert, S.; Werner, J.; Jess, I.; Näther, C. Influence of metal coordination and co-ligands on the magnetic properties of 1D Co(NCS)₂ coordination polymers. *Phys. Chem. Chem. Phys.* **2017**, *19*, 3232–3243. [[CrossRef](#)]
6. Werner, J.; Tomkowicz, Z.; Rams, M.; Ebbinghaus, S.G.; Neumann, T.; Näther, C. Synthesis, structure and properties of [Co(NCS)₂(4-(4-chlorobenzyl)pyridine)₂]_n, that shows slow magnetic relaxations and a metamagnetic transition. *Dalton Trans.* **2015**, *44*, 14149–14158. [[CrossRef](#)]
7. Werner, J.; Rams, M.; Tomkowicz, Z.; Runcevski, T.; Dinnebier, R.E.; Suckert, S.; Näther, C. Thermodynamically metastable thiocyanato coordination polymer that shows slow relaxations of the magnetization. *Inorg. Chem.* **2015**, *54*, 2893–2902. [[CrossRef](#)] [[PubMed](#)]
8. Louka, F.R.; Massoud, S.S.; Haq, T.K.; Koikawa, M.; Mikuriya, M.; Omote, M.; Fischer, R.C.; Mautner, F.A. Synthesis, structural characterization and magnetic properties of one-dimensional Cu(II)-azido coordination polymers. *Polyhedron* **2017**, *138*, 177–184. [[CrossRef](#)]

9. Massoud, S.S.; Henary, M.M.; Maxwell, L.; Martín, A.; Ruiz, E.; Vicente, R.; Fischer, R.C.; Mautner, F.A. Structure, magnetic properties and DFT calculations of azido-copper(II) coordination compounds with different azido-bonding, nuclearity and dimensionality. *New J. Chem.* **2018**, *42*, 2627–2639. [[CrossRef](#)]
10. Mautner, F.R.; Traber, M.; Fischer, R.C.; Torvisco, A.; Reichmann, K.; Speed, S.; Vicente, R.; Massoud, S.S. Thiocyanato-4-methoxypyridine-cobalt(II) coordination compounds with diverse geometries and a bridged 1D coordination polymer showing metamagnetic transition. *Polyhedron* **2018**, *154*, 436–442. [[CrossRef](#)]
11. Massoud, S.S.; Louka, F.R.; Obaid, Y.K.; Vicente, R.; Ribas, J.; Fischer, R.C.; Mautner, F.A. Metal ions directing the geometry and nuclearity of azido-metal(II) coordination compounds derived from bis(2-(3,5-dimethyl-1H-pyrazol-1-yl)ethyl)-amine. *Dalton Trans.* **2013**, *42*, 3968–3978. [[CrossRef](#)] [[PubMed](#)]
12. Mautner, F.A.; Louka, F.R.; Hofer, J.; Spell, M.; Lefèvre, A.; Guilbeau, A.E.; Massoud, S.S. One-dimensional cadmium polymers with alternative di(EO/EE) and di(EO/EO/EO/EE) bridged azide bonding modes. *Cryst. Growth Des.* **2013**, *13*, 4518–4525. [[CrossRef](#)]
13. Świtlicka, A.; Czerwińska, K.; Machura, B.; Penkala, M.; Bieńko, A.; Bieńkod, D.; Zierkiewicz, W. Thiocyanate copper coordination compounds with pyrazole-derived ligands—Synthesis, crystal structures, DFT calculations and magnetic properties. *CrystEngComm* **2016**, *18*, 9042–9055. [[CrossRef](#)]
14. Mukherjee, S.; Mukherjee, P.S. Versatility of azide in serendipitous assembly of copper(II) magnetic polyclusters. *Acc. Chem. Res.* **2013**, *46*, 2556–2566. [[CrossRef](#)] [[PubMed](#)]
15. Adhikary, C.; Koner, S. Structural and magnetic studies on copper(II) azido coordination compounds. *Coord. Chem. Rev.* **2010**, *254*, 2933–2958. [[CrossRef](#)]
16. Zeng, Y.-F.; Hu, X.; Liu, F.-C.; Bu, X.-H. Azido-mediated systems showing different magnetic behaviors. *Chem. Soc. Rev.* **2009**, *38*, 469–480. [[CrossRef](#)] [[PubMed](#)]
17. Kettenmann, S.D.; Louka, F.R.; Marine, E.; Fischer, R.C.; Mautner, F.A.; Kulak, N.; Massoud, S.S. Efficient artificial nucleases for mediating DNA cleavage based on tuning the steric effect in the pyridyl derivatives of tripod tetraamine-cobalt(II) coordination compounds. *Eur. J. Inorg. Chem.* **2018**, *20–21*, 2322–2338. [[CrossRef](#)]
18. Massoud, S.S.; Perkins, R.S.; Louka, F.R.; Xu, W.; Le Roux, A.; Dutercq, Q.; Fischer, R.C.; Mautner, F.A.; Handa, M.; Hiraoka, Y.; et al. Efficient hydrolytic cleavage of plasmid DNA by chloro-cobalt(II) coordination compounds based on sterically hindered pyridyl tripod tetraamine ligands: Synthesis, crystal structure and DNA cleavage activity. *Dalton Trans.* **2014**, *43*, 10086–10103. [[CrossRef](#)]
19. Massoud, S.S.; Ledet, C.C.; Junk, T.; Bosch, S.; Comba, P.; Herchel, R.; Hošek, J.; Trávníček, Z.; Fischer, R.C.; Mautner, F.A. Dinuclear metal(II)-acetato coordination compounds based on bicompartamental 4-chlorophenol: Synthesis, structure, magnetic properties, DNA interaction and phosphodiester hydrolysis. *Dalton Trans.* **2016**, *45*, 12933–12950. [[CrossRef](#)]
20. Massoud, S.S.; Louka, F.R.; Xu, W.; Perkins, R.; Vicente, R.; Albering, J.H.; Mautner, F.A. DNA cleavage by structurally characterized dinuclear copper(II) coordination compounds based on triazine. *Eur. J. Inorg. Chem.* **2011**, *23*, 3469–3479. [[CrossRef](#)]
21. Youngme, Y.; Phatchimkun, J.; Suksangpanya, U.; Pakawatchai, C.; van Albada, G.A.; Quesada, M.; Reedijk, J. A new unique tetranuclear Cu(II) compound with double bridging thiocyanate anions: Synthesis, X-ray structure and magnetism of $[\text{Cu}_4(\mu_{1,3}\text{-NCS})_6(\text{dpyam})_4(\text{O}_2\text{CH})_2(\text{H}_2\text{O})_2]$ (dpyam = di-2-pyridylamine). *Inorg. Chem. Commun.* **2006**, *9*, 242–247. [[CrossRef](#)]
22. Trofimenko, S.; Calabrese, J.C.; Kochi, J.K.; Wolowicz, S.; Hulsbergen, F.B.; Reedijk, J. Spectroscopic analysis, coordination geometry, and x-ray structures of nickel(II) compounds with sterically demanding tris(pyrazolyl)borate ligands and azide or (thio)cyanate anions. Crystal and molecular structures of bis[(μ -thiocyanato-N,S)(hydrotris(3-isopropyl-4-bromopyrazol-1-yl)borato)nickel(II)]-3-heptane and (thiocyanato-N)(hydrotris(3-tert-butyl-5-methylpyrazol-1-yl)borato)nickel(II). *Inorg. Chem.* **1992**, *31*, 3943–3950.
23. Maity, D.; Chattopadhyay, S.; Ghosh, A.; Drew, M.G.B.; Mukhopadhyay, G. Syntheses, characterization and X-ray crystal structures of a mono- and a penta-nuclear nickel(II) coordination compound with oximate Schiff base ligands. *Inorg. Chim. Acta* **2011**, *365*, 25–31. [[CrossRef](#)]
24. Bhowmik, P.; Chattopadhyay, S.; Drew, M.G.B.; Diaz, C.; Ghosh, A. Synthesis, structure and magnetic properties of mono- and di-nuclear nickel(II) thiocyanate coordination compounds with tridentate N₃ donor Schiff bases. *Polyhedron* **2010**, *29*, 2637–2642. [[CrossRef](#)]
25. Carranza, J.; Sletten, J.; Lloret, F.; Julve, M. Preparation, crystal structures and magnetic properties of three thiocyanato-bridged copper(II) coordination compounds with 2,2'-biimidazole or 2-(2'-pyridyl)imidazole as terminal ligands. *Polyhedron* **2009**, *28*, 2249–2257. [[CrossRef](#)]

26. Maji, T.K.; Mostafa, G.; Clemente-Juan, J.M.; Ribas, J.; Lloret, F.; Okamoto, K.; Chaudhuri, N.R. Synthesis, crystal structure and magneto-structural correlation of an unusual thiocyanato-bridged nickel(II) compound, $[\text{Ni}(\mu\text{-NCS})(\text{dpt})(\text{NCS})]_2[\text{Ni}(\mu\text{-NCS})(\text{dpt})(\text{NCS})]_4$ [dpt = bis(3-aminopropyl)amine]. *Eur. J. Inorg. Chem.* **2003**, 1005–1011. [[CrossRef](#)]
27. Monfort, M.; Ribas, J.; Solans, X. Crystal structures and ferromagnetic properties of two new dinuclear coordination compounds with thiocyanato bridging Ligands: $[\text{Ni}_2(1,2\text{-diamino-2-methylpropane})_3(\text{NCS})_2]_2(\mu\text{-NCS})_2$ $[\text{Ni}(1,2\text{-diamino-2-methylpropane})_2(\text{NCS})_2]\cdot\text{H}_2\text{O}$ and $[\text{Ni}_2(1,2\text{-diamino-2-methylpropane})_4](\mu\text{-NCS})_2(\text{PF}_6)_2$. Magneto-structural correlations. *Inorg. Chem.* **1994**, 33, 4271–4276.
28. Massoud, S.S.; Guilbeau, A.E.; Luong, H.T.; Vicente, R.; Albering, J.H.; Fischer, R.C.; Mautner, F.A. Mononuclear, dinuclear and polymeric 1-D thiocyanato- and dicyanamido-copper(II) coordination compounds based on tridentate coligands. *Polyhedron* **2013**, 54, 26–33. [[CrossRef](#)]
29. Massoud, S.S.; Mautner, F.A. Synthesis and Structure determination of two new dinuclear end-to-end doubly bridged azido- and thiocyanato-copper(II) coordination compounds derived from diethyldiethylenetriamine. *Inorg. Chim. Acta* **2005**, 358, 3334–3340. [[CrossRef](#)]
30. Mautner, F.A.; Louka, F.R.; Gallo, A.A.; Saber, M.R.; Burham, N.B.; Albering, J.H.; Massoud, S.S. Thiocyanato-Cu(II) coordination compounds derived from tridentate amine ligand and from alanine. *Transit. Met. Chem.* **2010**, 35, 613–619. [[CrossRef](#)]
31. Mautner, F.A.; Vicente, R.; Massoud, S.S. Structure Determination of Nitrito- and Thiocyanato-copper(II) Coordination compounds. X-ray Structures of $[\text{Cu}(\text{Medpt})(\text{ONO})(\text{H}_2\text{O})]\text{ClO}_4$ (1), $[\text{Cu}_2(\text{dien})(\text{ONO})_2]\text{ClO}_4$ (2) and $[\text{Cu}_2(\text{Medpt})_2(\mu_{\text{N,S}}\text{-NCS})_2](\text{ClO}_4)_2$ (3) (Medpt = 3,3'-diamino-N-methyl-dipropylamine and dien = diethylenetriamine). *Polyhedron* **2006**, 25, 1673–1680.
32. Wriedt, M.; Näther, C. Dimorphic modifications of the thiocyanato-bridged coordination polymer $[\text{Ni}(\text{NCS})_2(\text{pyridazine})(\text{H}_2\text{O})_{0.5}]_n$ with different magnetic properties. *Eur. J. Inorg. Chem.* **2011**, 228–234. [[CrossRef](#)]
33. You, Z.-L.; Zhu, H.-L. Syntheses, crystal structures, and antibacterial activities of four Schiff base coordination compounds of copper and zinc. *Z. Anorg. Allg. Chem.* **2004**, 630, 2754–2760. [[CrossRef](#)]
34. Ding, B.; Huang, Y.Q.; Liu, Y.Y.; Shi, W.; Cheng, P. Synthesis, structure and magnetic properties of a novel 1D coordination polymer $\{[\text{Cu}_2(\text{amtrz})_4(1,1\text{-}\mu\text{-NCS})_2](\text{ClO}_4)_2\cdot\text{H}_2\text{O}\}_n$. *Inorg. Chem. Commun.* **2007**, 10, 7–10. [[CrossRef](#)]
35. Hou, L.; Li, D.; Shi, W.-J.; Yin, Y.-G.; Ng, S.W. Ligand-controlled mixed-valence copper rectangular grid-type coordination polymers based on pyridylterpyridine. *Inorg. Chem.* **2005**, 44, 7825–7832. [[CrossRef](#)] [[PubMed](#)]
36. Depree, C.V.; Beckmann, U.; Heslop, K.; Brooker, S. Monomeric, trimeric and polymeric assemblies of dicopper(II) coordination compounds of a triazolate-containing Schiff-base macrocycle. *J. Chem. Soc. Dalton Trans.* **2003**, 3071–5081. [[CrossRef](#)]
37. Hao, Z.-M.; Liu, H.-P.; Han, H.-H.; Wang, W.-T.; Zhang, X.-M. A luminescent $[\text{Ag}_3\text{S}_3]_n$ -tube based metal-organic framework. *Inorg. Chem. Commun.* **2009**, 12, 375–377. [[CrossRef](#)]
38. Legendre, A.O.; Mauro, A.E.; Ferreira, J.G.; Ananias, S.R.; Santos, R.H.A.; Netto, A.V.G. A 2D coordination polymer with brick-wall network topology based on the $[\text{Cu}(\text{NCS})_2(\text{pn})]$ monomer. *Inorg. Chem. Commun.* **2007**, 10, 815–820. [[CrossRef](#)]
39. Lin, J.-D.; Li, Z.-H.; Li, J.-R.; Du, S.-W. Synthesis and crystal structures of three novel coordination polymers generated from AgCN and AgSCN with flexible N-donor ligands. *Polyhedron* **2007**, 26, 107–114. [[CrossRef](#)]
40. Krautscheid, H.; Emig, N.; Klaassen, N.; Seringer, P. Thiocyanato coordination compounds of the coinage metals: Synthesis and crystal structures of the polymeric pyridine coordination compounds $[\text{Ag}_x\text{Cu}_y(\text{SCN})_x + y(\text{py})_z]$. *J. Chem. Soc. Dalton Trans.* **1998**, 3071–3078. [[CrossRef](#)]
41. Shriver, S.; Weller, M.; Overton, T.; Rourke, J.; Armstrong, F. *Inorganic Chemistry*, 6th ed.; W.H. Freeman and Company: New York, NY, USA, 2014; pp. 139–141.
42. Mautner, F.A.; Albering, J.H.; Harrelson, E.V.; Gallo, A.A.; Massoud, S.S. N-bonding vs. S-bonding in Thiocyanato-copper(II) coordination compounds. *J. Mol. Struct.* **2011**, 1006, 570–575.
43. Mautner, F.A.; Louka, F.R.; Le Guet, T.; Massoud, S.S. Pseudohalide copper(II) complexes derived from polypyridyl ligands. Synthesis and characterization. *J. Mol. Struct.* **2009**, 919, 196–203. [[CrossRef](#)]
44. Geary, W.J. The use of conductivity measurements in organic solvents for the characterization of coordination compounds. *Coord. Chem. Rev.* **1971**, 7, 81–122. [[CrossRef](#)]

45. Hathaway, B.J.; Wilkinson, G.; Gillard, R.D.; McCleverty, J.A. (Eds.) *Comprehensive Coordination Chemistry*; Pergamon Press: Oxford, UK, 1987; Volume 5, p. 533.
46. Näther, C.; Wöhlert, S.; Boeckmann, J.; Wriedt, M.; Jeß, I. A rational route to coordination polymers with condensed networks and cooperative magnetic properties. *Z. Anorg. Allg. Chem.* **2013**, *639*, 2696–2714. [[CrossRef](#)]
47. Mautner, F.A.; Fischer, R.C.; Rashmawi, L.G.; Louka, F.R.; Massoud, S.S. Structural characterization of metal(II) thiocyanato coordination compounds derived from bis(2-(1-H-pyrazol-1-yl)ethyl)amine. *Polyhedron* **2017**, *124*, 237–242. [[CrossRef](#)]
48. Massoud, S.S.; Louka, F.R.; David, R.N.; Dartez, M.J.; Nguyn, Q.L.; Labry, N.J.; Fischer, R.C.; Mautner, F.A. Five-coordinate thiocyanato- and azido-metal(II) coordination compounds based pyrazolyl ligands. *Polyhedron* **2015**, *90*, 258–265. [[CrossRef](#)]
49. Massoud, S.S.; Le Quan, L.; Gatterer, K.; Albering, J.H.; Fischer, R.C.; Mautner, F.A. Structural Characterization of five-coordinate copper(II), nickel(II), and cobalt(II) thiocyanato coordination compounds derived from bis(2-(3,5-dimethyl-1-pyrazolyl)ethyl)amine. *Polyhedron* **2012**, *31*, 601–606. [[CrossRef](#)]
50. Mautner, F.A.; Landry, K.N.; Gallo, A.A.; Massoud, S.S. Molecular structure of mononuclear azido- and diacyanamido-Cu(II) coordination compounds. *J. Mol. Struct.* **2007**, *837*, 72–78. [[CrossRef](#)]
51. Shriver, E.; Weller, M.; Overton, T.; Rourke, J.; Armstrong, F. *Inorganic Chemistry*, 6th ed.; W.H. Freeman and Company: New York, NY, USA, 2014; pp. 536–540.
52. Pervukhina, N.V.; Podberezkaya, N.V.; Kirichenko, N.V. Crystal structure of isothiocyanatobis(ethylenediamine) copper(II) bromide [Cu(en)₂(NCS)]Br. *J. Struct. Chem.* **1982**, *23*, 130–133. [[CrossRef](#)]
53. Cannas, M.; Carta, G.; Marongiu, G. Crystal structures of thiocyanate polyaminecopper(II) coordination compounds. Part I. Bis(ethylenediamine)-copper(II) thiocyanate perchlorate. *J. Chem. Soc. Dalton Trans.* **1973**, *3*, 251–254. [[CrossRef](#)]
54. Brown, B.W.; Lingafelter, E.C. The crystal structure of bis(ethylenediamine)copper(II) thiocyanate. *Acta Crystallogr.* **1964**, *17*, 254–259. [[CrossRef](#)]
55. Koman, M.; Macaskova, L.; Ondrejovic, G.; Koren, B.; Battaglia, L.; Corradi, A. Structure of bis(ethylenediamine) isothiocyanato(copper(II) tetrafluoroborate, violet isomer. *Acta Crystallogr.* **1988**, *C44*, 245–246.
56. Garaj, J.; Dunaj-Jurco, M.; Lindgren, O. The thiocyanate group as ligand in copper coordination compounds the structure of the dithiocyanate ethylenediamine copper(II) coordination compound. *Collect. Czech. Chem. Commun.* **1971**, *36*, 3863–3873. [[CrossRef](#)]
57. Andreotti, G.D.; Cavalca, L.; Sgarabotto, P. Metal chelates of 1,3-diaminopropane. 1. Crystal and molecular structure of bis(1,3-diaminopropane)copper(II) thiocyanate. *Gazz. Chim. Ital.* **1971**, *101*, 483–492.
58. Cannas, M.; Carta, G.; Marongiu, G. Crystal structures of thiocyanate polyaminecopper(II) coordination compounds. Part II. Bis-(1,3-diaminopropane)-isothiocyanatocopper(II) perchlorate. *J. Chem. Soc. Dalton Trans.* **1974**. [[CrossRef](#)]
59. Kovenranta, J.; Pajunen, A. Crystal structure of bis(*N,N'*-dimethylethylenediamine)copper(II) thiocyanate. *Suom. Kemistil. B* **1970**, *45*, 119–123.
60. Xu, Q.; Du, M.; Song, Z.-R.; Guo, Y.-M.; Bu, X.-H. Synthesis, characterization and crystal structure of a DACO-Cu- μ -SCN coordination compound (DACO = 1,5-diazacyclooctane). *Chin. J. Inorg. Chem.* **2005**, *21*, 109–112.
61. Wang, L.-H.; Li, L.-Z. catena-Poly[[(*N,N*-diethylethane-1,2-diamine)thiocyanatocopper(II)]- μ -thiocyanato]. *Acta Crystallogr.* **2007**, *63*, m1214–m1216. [[CrossRef](#)]
62. Espinosa, A.; Sohail, M.; Habib, M.; Naveed, K.; Saleem, M.; Rehman, H.; Hussain, I.; Munavar, A.; Ahmad, S. Synthesis, crystal structure, theoretical calculations, and electrochemical and biological studies of polymeric (*N,N,N',N'*-tetramethylethylenediamine)bis(thiocyanato- κ N)copper(II), [Cu(tmEDA)(NCS)₂]_n. *Polyhedron* **2015**, *90*, 252–257. [[CrossRef](#)]
63. Wang, C.-Y. catena-Poly[[(*N,N*-di-methyl-propane-1,3-di-amine)thiocyanato-copper(II)]- μ -thio-cyanato]. *Acta Crystallogr.* **2007**, *63*, m832–m834.
64. Wang, Z.-D.; Han, W.; Bian, F.; Liu, Z.-Q.; Yan, S.-P.; Liao, D.-Z.; Jiang, Z.-H.; Cheng, P. Synthesis, X-ray structure, spectroscopic and magnetic properties of [Cu(DACO)(μ -1,1-N₃)(μ -1,3-N₃)_n] and [Cu(DACO)(μ -NCS)(NCS)]_n (DACO = 1,5-diazacyclooctane). *J. Mol. Struct.* **2005**, *733*, 125–131. [[CrossRef](#)]
65. Vrabel, V.; Garaj, J.; Sivý, J.; Oktavec, D. Aquadiisothiocyanato(*N,N,N',N'*-tetramethylethylenediamine-*N,N'*) copper(II). *Acta Crystallogr.* **1999**, *C55*, 551–553. [[CrossRef](#)]

66. Pajunen, A.; Hamalainen, R. The crystal structure of bis(*N*-methylethylenediamine)copper(II) thiocyanate. *Suom. Kemistil. B* **1972**, *45*, 122–129.
67. Sheldrick, G.M. *SADABS Version 2*; University of Goettingen: Wilhelmsplatz, Germany, 2001.
68. Sheldrick, G.M. A short history of SHELX. *Acta Crystallogr.* **2008**, *A64*, 112–122. [[CrossRef](#)] [[PubMed](#)]
69. Macrae, C.F.; Edington, P.R.; McCabe, P.; Pidcock, E.; Shields, G.P.; Taylor, R.; Towler, T.; van de Streek, J. Mercury: Visualization and analysis of crystal structures. *J. Appl. Crystallogr.* **2006**, *39*, 453–457. [[CrossRef](#)]
70. Müller, P.; Herbst-Irmer, R.; Spek, A.L.; Schneider, T.R.; Sawaya, M.R. *Crystal Structure Refinement: A Crystallographers's Guide to SHELXL*; Oxford University Press: Oxford, UK, 2006.
71. Kim, K.; Jordan, K.D. Comparison of density functional and MP2 calculations on the water monomer and dimer. *J. Phys. Chem.* **1998**, *40*, 10089–10094. [[CrossRef](#)]
72. Hehre, W.J.; Ditchfield, R.; Stewart, R.F.; Pople, J.A. Self-consistent molecular orbital methods. IV. Use of Gaussian expansions of Slater-type orbitals. Extension to second-row molecules. *J. Chem. Phys.* **1970**, *52*, 2769–2773. [[CrossRef](#)]
73. Frisch, M.J.; Trucks, G.W.; Schlegel, H.B.; Scuseria, G.E.; Robb, M.A.; Cheeseman, J.R.; Scalmani, G.; Barone, V.; Petersson, G.A.; Nakatsuji, H.; et al. *Gaussian 03, Revision C02*; Gaussian, Inc.: Wallingford, CT, USA, 2016.
74. Handy, J.V.; Ayala, G.; Pike, R.D. Structural comparison of copper(II) thiocyanate pyridine complexes. *Inorg. Chim. Acta* **2017**, *456*, 64–75. [[CrossRef](#)]
75. Costamagna, J.; Caruso, F.; Vargas, J.; Manriquez, V. Planar or tetrahedral coordination in copper(II) coordination compounds induced by bromo substitution. *Inorg. Chim. Acta* **1998**, *267*, 151–158. [[CrossRef](#)]
76. Shimizu, I.; Morimoto, Y.; Faltermeier, D.; Kerscher, M.; Paria, S.; Abe, T.; Sugimoto, H.; Fujieda, N.; Asano, K.; Suzuki, T.; et al. Tetrahedral copper(II) coordination compounds with a labile coordination site supported by a tris-tetramethylguanidinato ligand. *Inorg. Chem.* **2017**, *56*, 9634–9645. [[CrossRef](#)]



© 2019 by the authors. Licensee MDPI, Basel, Switzerland. This article is an open access article distributed under the terms and conditions of the Creative Commons Attribution (CC BY) license (<http://creativecommons.org/licenses/by/4.0/>).